ISSN 0915-633X

NATIONAL INSTITUTE FOR FUSION SCIENCE

Collisionless Pitch Angle Scattering of Plasma Ions at the Edge Region of an FRC

T. Takahashi, Y. Tomita, H. Momota and Nikita V. Shabrov

(Received - May 26, 1997)

NIFS-497 July 1997

RESEARCH REPORT
NIFS Series

NAGOYA, JAPAN

Collisionless Pitch Angle Scattering of Plasma Ions at the Edge Region of an FRC

Toshiki Takahashi,
The Graduate University for Advanced Studies, Toki-shi, Gifu 509-52, Japan

Yukihiro Tomita, Hiromu Momota,
The Graduate University for Advanced Studies, Toki-shi, Gifu 509-52, Japan
and National Institute for Fusion Science, Toki-shi, Gifu 509-52, Japan

and Nikita V. Shabrov
Moscow State Technical University, P.O.Box 38, Moscow 105007, Russia

Keywords: FRC, D-^{3}He Fusion, Action Integral, Pitch Angle Scattering

Collisionless Pitch Angle Scattering of Plasma Ions at the Edge Region of an FRC

Toshiki Takahashi,
The Graduate University for Advanced Studies, Toki-shi, Gifu 509-52, Japan

Yukihiro Tomita, Hiromu Momota,
The Graduate University for Advanced Studies, Toki-shi, Gifu 509-52, Japan
and National Institute for Fusion Science, Toki-shi, Gifu 509-52, Japan

and Nikita V. Shabrov
Moscow State Technical University, P.O.Box 38, Moscow 105007, Russia

Abstract

Motion of a plasma ion gyrating around the separatrix of a field-reversed configuration is studied. Numerical studies showed that action integral of a particle changes abruptly when a particle passes through the vicinity of a field null x-point. This phenomena is understood as collisionless stochastic scattering of pitch angle. In case of a particle with positive canonical angular momentum P_θ , resultant correlation coefficients of action integral between before and after the scattering appear to be stochastic in some cases. As action integral increases for a particle with negative P_θ , its motion tends to be adiabatic. If negative P_θ of a particle approaches to zero, a stochastic motion is observed.

1. Introduction

A field-reversed configuration (FRC) is one of the most promising confinement system of plasma to bring out attractive characteristics in a D-^{3}He fueled fusion (1,2). A high beta value (> 0.9) of an FRC (3 - 5) extremely reduces synchrotron radiation loss from plasma with high temperature of around 100 keV which is required to burn D-^{3}He fueled plasma (1,2). The open magnetic fields surrounding burning plasma of an FRC enable us to install direct energy converters with high conversion efficiency (6,7). This brings about a commercial fusion reactor with high plant efficiency. Because of low neutron yield from D-^{3}He fusion a commercial reactor is expected as intrinsically safe and environmentally acceptable in view of disposal of radioactive waste (8). These attractive characteristics have been shown clearly on a conceptual design of a commercial fusion reactor ARTEMIS (9,10) on the bases of an FRC with D-^{3}He fusion fuel. In order to advance fusion research toward this direction understanding of plasma in an FRC, especially plasma transport, is one of the most important key issues. In this paper we investigate behavior of particles near the separatrix of an FRC. Results from this study give the physical bases to clarify loss mechanisms in an FRC.

A stationary and axisymmetric plasma in a field-reversed configuration (FRC) has been described traditionally in terms of the Hamiltonian H and the canonical angular momentum P_θ . Hsiao et al.(11-13) have discussed particle confinement in the edge region of an FRC by introducing the accessible region expressed as a function of H and P_θ . They assumed that a particle is confined within the separatrix of an FRC, if its accessible region exists inside the separatrix. On the contrary, a particle will be lost immediately if the associated accessible region is open to a magnetic mirror point. Their discussions are based on Finn's paper(14) or on the fact that some particles describe ergodic trajectories in their accessible regions. Finn et al. have concerned orbits of ion rings and concluded that the trajectories of ion rings appear to be stochastic as their energies increase. Since an ergodic particle travels any point in the accessible region, loss characteristics of the particle in an FRC are described by the variables H and P_θ through the accessible region. This result is rather a restricted one, however, because the ergodic assumption will hold only for a special kind of particles.

It is insufficient to describe the particle motion in terms of only the accessible region or variables H and P_θ , if the motion is non-ergodic. Indeed, in a case where a particle exhibits a regular gyrating motion, an additional constant of motion such as the magnetic moment is required to describe the motion, because it indicates the motion along the line of force and determines the particle loss through the mirror point.

The magnetic moment is a useful concept to characterize the particle trajectory in a regular magnetic field. Nevertheless, it is not adequate to describe a motion of a particle in an FRC because the magnetic field vanishes at an x-point. An adequate constant of motion is, therefore, required to characterize particles in an FRC. A field-null x-point locates at the edge region of an FRC, where behavior of a particle appears to be irregular and the adiabatic invariance will be violated. In this paper, behavior of a particle in the edge region of an FRC will be studied to reveal the violating process in a certain constant of motion.

The organization of this paper is as follows: In Sec.2, the accessible region near the separatrix of an FRC is introduced. The action integral of a particle near the separatrix is defined as an additional variable characterizing the motion, and its time behavior is presented in Sec.3. Results from numerical calculations on pitch angle scattering and related collisionless loss of plasma ions will be presented in Sec.4. Sec.5 is devoted to summarize the conclusions.

2. Accessible Regions

The Hamiltonian of a charged particle in an axisymmetric magnetic field has the form in the cylindrical coordinates system:

$$H \equiv \frac{P_r^2}{2M} + \frac{P_z^2}{2M} + \frac{\{P_\theta - q\psi(r,z)\}^2}{2r^2 M}. \tag{1}$$

Here, quantities M, q, and P_θ denote respectively the mass, the charge, and the canonical angular momentum of an ion. We have ignored the scalar potential, for the simplicity, in the present paper. An electrostatic potential plays an important role in the ambipolar particle diffusion, however, that will be discussed in the subsequent paper.

The quantity $\psi(r,z)$ is the magnetic flux function defined by $\int B_z\, r dr$, and is obtainable as a solution to the equation:

$$r\frac{\partial}{\partial r}\left(\frac{1}{r}\frac{\partial \psi}{\partial r}\right) + \frac{\partial^2 \psi}{\partial z^2} = -\mu_0 r J_\theta\ . \tag{2}$$

As a solution to the Eq.(2), we will employ Hill's vortex[15] inside the separatrix. Accordingly, the current density J_θ in the azimuthal direction is proportional to the radial position r from the z-axis inside the separatrix and zero outside the separatrix. The vacuum magnetic field outside the separatrix is obtained by putting zero current density in the Eq.(2) and by connecting to the inner Hill's vortex solution smoothly at the separatrix. The boundary condition at the metallic wall ($r = r_w$) for the solution to Eq.(2) depends also on the mirror coils. The mirror ratio (maximum $B_{z(r=r_w)}$ / minimum $B_{z(r=r_w)}$) is chosen as 4.0 in the present paper. Since the direction of the magnetic field outside the separatrix of an FRC is opposite to the z-axis, the sign of the flux function outside the separatrix is negative. We have to note, here, that our choice of the magnetic configuration has no physical base. The physical discussion based on this configuration seems, however, essentially valid even in a general case.

In a stationary and axisymmetric field, both the Hamiltonian H and the canonical angular momentum P_θ of an ion are constants of motion. Then we are able to define an accessible region, inside which an ion with a set of constants of motion exists. The expression for defining the accessible region is:

$$-\sqrt{2MH} \leq \frac{P_\theta - q\psi(r,z)}{r} \leq \sqrt{2MH}\,. \tag{3}$$

This equation is equivalent to the condition that the quantity $P_r^2 + P_z^2$ is non negative.

If a positive canonical angular momentum of an ion approaches to zero, the associated accessible region is close to or involves a part of the separatrix. In this case, the accessible region extends toward the mirror point as is exhibited in Fig. 1(a). In this figure, the typical value of the ion temperature is chosen as 100keV. Other parameters are chosen as follows: The separatrix radius and the half length of the separatrix is 1.68m and 3.89m, respectively. The magnetic field at the separatrix on the midplane is 5.3T. The accessible region shown in Fig. 1(a) is characterized by a particle motion near the field-null x-point that is similar to a magnetic cusp point. We call, therefore, this type of accessible region as the cusp-like accessible region, or simply as *the cusp-like region*. The cusp-like region has three branches. One is located around the separatrix and away from the z-axis on the midplane (hereinafter referred to *the separatrix-part*). The second branch is situated around the z-axis inside the separatrix. Since, the direction of the field line in this area is opposite to the external magnetic field, we will refer this branch as *the reversal-part*. The other branch extends toward the mirror end (hereinafterrefer as *the mirror-part*).

On the other hand, in the case that a particle has a large negative canonical angular momentum, one watches a different shape of the accessible region. We can find a typical shape of this accessible region in Fig. 1(b). In this case, we find no accessible region near the z-axis inside the separatrix. A particle in this region is always off-axis and gyrating, similar to that in the simple magnetic mirror. We will call the accessible region of this type as the mirror-like accessible region, or simply as *the mirror-like region* in the present paper.

As is discussed previously, we have to find a parameter convenient to characterize the axial motion corresponding to the pitch angle or the magnetic moment of an ion in a magnetic mirror. An FRC will be immersed in a magnetic mirror and the magnetic field is uniform near the separatrix on the midplane or near the mirror point. Accordingly, we are able to describe the behavior of ions in terms of the magnetic moment as well as the Hamiltonian and the canonical angular momentum at these regions. Unfortunately, the magnetic moment is unable to define near an x-point where non-adiabatic motion is dominant in the dynamics. As a result, it is better to introduce another variable to characterize the axial motion of an ion: The action integral that will be discussed in the following section.

3. Behavior of the Action Integral

An introduction of the action integral J defined by:

$$J \equiv \frac{1}{2\pi} \oint P_r \, dr \tag{4}$$

will help us to describe the axial motion of an ion in an FRC. Integration by r in Eq.(4) has to be completed over a whole cycle of radial displacement of the ion. An ion with a larger J has a larger radial motion, or in other words a smaller axial motion. If an ion has a sufficiently small J, it will reach the axial end, and eventually, it suffers from a particle loss through a magnetic mirror. From this viewpoint, the quantity J can be applicable even for the analysis of the particle loss in a magnetic mirror, instead of the magnetic moment. The magnetic moment can be defined only in the relatively uniform magnetic field. In the edge region as shown in Fig.1(a), the magnetic field of an FRC satisfies this condition except for at the vicinity of x-points. When the magnetic moment μ of an ion can be defined, it relates with the action integral J by the formulas:

$$\begin{aligned} J &= \frac{M}{q}\mu, && \text{for off-axis gyrating particles} \\ J &= \left(\frac{d}{\rho}\right)^2 \frac{M}{q}\mu. && \text{for encircling particles} \end{aligned} \tag{5}$$

The gyro-radius and the radial distance of the gyrating center from the z-axis of the ion are denoted by ρ and d, respectively. The first equation of (5) describes the relation of an off-axis gyrating ion. On the other hand, an ion with positive P_θ moving around the z-axis at the mirror end is encircling, and the relation between J and the magnetic moment for this ion is described by the second equation.

The action integral J can be applicable to discuss the particle loss of an FRC, because its definition holds valid even near a field-null x-point. The loss criterion of particles in a magnetic mirror with vanishing electrostatic potential is $\mu < \mu_m$, where the quantity μ_m denotes the critical magnetic moment for the mirror loss. This criterion is valid for an off-axis gyrating ion but not for an encircling ion. Encircling loss ions can not be characterized by a smaller μ but a smaller J. Thus, the criterion $\mu < \mu_m$ is insufficient to describe loss of ions in an FRC. Application of the action integral gives a simple formula for the particle loss, i.e., the action integral of an encircling ion that is attainable at the mirror point is a smaller one (small d), that criterion is held even for an off-axis gyrating ion whose action integral is proportional to the magnetic moment.

The action integral will be constant if an ion is traveling at a uniform magnetic field. While, it changes as the ion passes through the domain of an x-point. An example of the time history of the action integral for an ion (Fig.2) verifies the phenomena. This behavior of the action integral advocates its applicability for the kinetic theory to be a useful tool. An abrupt step-like change in the action integral, however, is observed when an ion goes through the domain of an x-point. The trajectory changes instantaneously from off-axis gyrating to encircling betatron or figure-8 trajectory, and vice versa. Accordingly, linear integration J along the trajectory might suffer from a rapid change. Since the amount of the change depends on the gyrating phase of the ion, the change in the action integral J is understood as stochastic. Quantitative discussions on the stochastic motion of an ion in the edge region of an FRC will be given in the next section. If an ion gets a small action integral at the mirror-part after suffering a change in the action integral, the ion will be lost through the magnetic mirror.

4. Collisionless Pitch Angle Scattering in the Vicinity of an X-point

In the previous section, we have shown an abrupt change in the action integral J. The action integral J keeps its value when an ion is traveling in a uniform magnetic field, while, it changes abruptly when the ion passes through the region where the magnetic field is weak such as in the vicinity of a field-null x-point. The process of this scattering was studied by using numerical calculations.

At the first subsection, we will discuss dynamics of ions in the cusp-like region. In the following subsection, we will discuss adiabaticity of an ion in the mirror-like region. An ion in the cusp-like region goes toward a branch in the three directions from an x-point. The typical appearance of the trajectory changes between an encircling betatron or a figure-8 trajectory and an off-axis gyrating one, depending on the branch. On the other hand, an ion in the mirror-like region is always off-axis gyrating. In this section, the ion is assumed to be a 100keV deuterium nucleus in the same configuration discussed in Sec.2. The particle loss associated to collisionless pitch angle scattering will be discussed in the last subsection.

4-1. cusp-like region

An ion in a cusp-like region has an action integral which is practically constant in respective branches, i.e., the separatrix-part, the reversal-part, and the mirror-part. Approaching to an x-point, however, the ion suffers from a certain change of the action integral abruptly. This ion sometimes changes its branch after passing through an x-point. For example, it transfers from the separatrix-part to the mirror-part. We call this process where an ion transfers from a certain branch to another branch as *the branch-transfer*.

[start up of the calculations]

Every ion in the cusp-like region goes through the vicinity of an x-point, because the Lorentz's force acting on a gyrating ion is directed to the x-point along a line of force. Therefore, in order to observe the changes in the action integral around an x-point, we will follow the motion of an ion, which starts at a certain point in the cusp-like region. The starting points and initial velocities of ions are given tentatively as follows:

i) A position z_i is tentatively chosen near an x-point.

ii) Radial positions r_i of respective particles are randomly chosen so as to be consistent with a given set of the Hamiltonian and the canonical angular momentum.

iii) The azimuthal component of velocity v_θ is determined from the definition of the canonical angular momentum as:

$$v_{\theta i} = \frac{1}{r_i M}\left(P_\theta - q\psi(r_i, z_i)\right), \tag{6}$$

and the initial values of v_{ri} and v_{zi} are

$$\begin{aligned} v_{ri} &= \sqrt{2H - v_{\theta i}^2}\,\sin\alpha, \\ v_{zi} &= \sqrt{2H - v_{\theta i}^2}\,\cos\alpha. \end{aligned} \tag{7}$$

The quantity α is the angle between the direction of the starting velocity and z-axis on the (r, z) plane. These velocity components v_{ri} and v_{zi} are given by giving the angle α, and then the values of corresponding action integral J can be obtainable.

In this calculation, ions are tentatively started at a given position z_i. Consequently, a value of the action integral J takes a restricted one, because the obtainable maximum value of the action integral J depends on the axial position z_i. Nevertheless, after suffering stochastic pitch angle scattering, ions will lose their initial memories except for the Hamiltonian and the canonical angular momentum and the eventual distribution of the action integral will be random. Thus the initial distribution of J can be seen as random, if we put the initial values of (r,z) and (v_r, v_θ, v_z) by those after pitch angle scattering.

[pitch angle scattering]

An ion with a positive canonical angular momentum is off-axis gyrating in the reversal-part and the separatrix-part of this cusp-like region. On the other hand, this ion is encircling in the mirror-part. Accordingly, if the ion suffers from a branch-transfer from the separatrix-part to the mirror-part, its trajectory also changes from off-axis gyrating to encircling. Since the action integral is a linear integral of the radial motion of the ion along its trajectory, it is inferred that the action integral changes due to the branch-transfer. In order to study the process of the branch-transfer quantitatively, we will calculate the correlation coefficient of the action integral between before and after the scattering. The correlation coefficient R of samples Xs is defined in terms of the average $\overline{X}$ and the dispersion V as:

$$R \equiv \frac{\overline{(\overline{X}_i - X_i)(\overline{X}_f - X_f)}}{\sqrt{V_i V_f}} . \tag{8}$$

The quantities with suffix i and f represent the quantities at the initial and final state, respectively. After an ion goes through a scattering region where the magnetic field is weak, the action integral J will keep their value at the new one. Values of J before and after the scattering are illustrated in Fig.3. Figures are separately presented by respective branch-transfers. The horizontal and the vertical axes are the action integral before and after the scattering, respectively. Since the maximum values of the action integral at the entrance to a branch differ in each branches, the range of axes are different in each figures. Based on these data, the correlation coefficients R of the action integral are obtained. The strong correlation of the action integral is observed when ions move from the separatrix-part to the same branch or from the reversal-part to the same branch. Negative correlation is found if an ion transfers its branch from the separatrix-part to the mirror-part or from the reversal-part to the separatrix-part. The strong correlation in the branch-transfer indicates that ions pass through an x-point without suffering from any appreciable stochastic pitch angle scattering.

The histograms of J after the first scattering and the second scattering are shown in Fig.4. The graphs show how many ions with a certain J will be presented in the subinterval after the scattering. If ions are subject to scattering isotropically, the distribution of J for off-axis gyrating ions after the scattering will be:

$$F(H, P_\theta, J) \propto \frac{1}{\sqrt{(H - |\Omega_s P_\theta|)/M - |\Omega_s| J}}. \tag{9}$$

The quantity Ω_f is the gyro-frequency of the ion at the exit of the scattering region. From the comparison between the histograms and analytical curves expressed by this equation, it appears that pitch angle scattering can be safely understood as the isotropic scattering process.

4-2. mirror-like region

An ion in the mirror-like region has a simple trajectory compared to that in the cusp-like region. Ions are always off-axis gyrating around a flux surface described as $P_\theta = q\psi(r, z)$, where azimuthal component of the velocity is zero. In other words, a gyrating center of an ion is on the flux surface characterized by the value P_θ. The situation is similar to that in a magnetic mirror system. Particle confinement in the magnetic mirror is generally described by using magnetic moment. Stochastic changes in magnetic moment will, however, often take place, as is predicted in many papers[(16-17)] for a case of a large mirror ratio. According to Chirikov[(17)], the adiabatic boundary on the J space depends on the mirror ratio, the gyro- radius, the pitch angle, and so on, and an analytical boundary for a case of a parabolic magnetic field was given analytically. In an FRC, on the other hand, the magnetic field along the gyrating center is quite different from that of a magnetic mirror and hard to obtain an analytical expression for the boundary. We employ, therefore, numerical studies to obtain the adiabatic boundary.

[calculation procedure]

The guiding center of ions moving in the mirror-like accessible region is on the surface described as $P_\theta = q\psi(r, z) : v_\theta = 0$. That is, the trace of the guiding center will change with the canonical angular momentum. As the absolute value of the canonical angular momentum $|P_\theta|$ increases, the trace of guiding center will gradually shifted from an x-point. In this situation, the point of the minimum magnetic field on the trace of the guiding center is located far from an x-point, and consequently, the ion motion will be approximately adiabatic. We will investigate the value of the action integral forming the adiabatic boundary and their dependence on canonical angular momentum. The energy of an ion is typically assumed to be 100keV in these calculation. The numerical calculations have been carried out as follows:

i) Several ions with the same canonical angular momentum P_θ are started to calculate the ensemble average.

ii) Initial positions and velocities are given as follows. All ions in the mirror-like region pass through the point of the minimum-field, therefore, we put the start point of ions at the place where the magnetic field is minimum. The magnetic field along the guiding center $B\ (z(r))$ is already known, and we find the axial position $z_0\ (r)$ where $dB\ (z\ (r))/dz = 0$. Several starting points are chosen near this point.

iii) The pitch angle (= $\tan^{-1}(v_{//}/v_{\perp})$) has to be given. The azimuthal velocity v_θ is already determined by Eq. (6), once the starting position of particle is given. Ions which start with a small pitch angle will be adiabatic. Therefore, we will investigate the adiabatic boundary from a particle moving perpendicular to the magnetic line of force and the pitch angle will be increased successively. When the position and the pitch angle of ions are fixed, then the radial and the axial components of the velocity are determined.

iv) The differences of action integrals ΔJ for ions with the same pitch angle are observed.

With these results, we are able to calculate the ensemble square average $<(\Delta J/J)^2>$. Note that if the value J is large or the motion is adiabatic, then the value of the ensemble square average $<(\Delta J/J)^2>$ is small.

If the ensemble square average is equal to $1/e^2$, then we will define the corresponding action integral as the adiabatic boundary. If the ensemble square average is larger than this value, the process can be understood as stochastic.

[adiabatic boundary]

The difference of the action integrals between the initial value of J and the one as it returns to the starting point are studied. We will consider a class of particles with the same pitch angle, and the ensemble mean square of $\Delta J/J$ are calculated with respect to these particles. The ensemble mean square $<(\Delta J/J)^2>$ as a functions of J is presented in Fig.5. When ions have a comparatively large action integral J , the ensemble mean square $<(\Delta J/J)^2>$ is small and the motion is adiabatic in this case. Adiabatic boundary is presented in Fig.6. One has to notify that extensive stochastic region is shown at small absolute value of P_θ, however, this region decreases as $|P_\theta|$ increases. It indicates that an ion exhibits a stochastic behavior when gyrating center is located in the vicinity of an x-point. On the other hand, an adiabatic behavior appears when gyrating center is located slightly away from an x-point. In this region the ratio of ion gyroradius to the separatrix radius is about 0.06.

4-3. collisionless loss of plasma ions

For an ion in the cusp-like region, if it suffers from pitch angle scattering and transferred into the mirror-part, it can be lost out of the end throat depending on the final value of J. According to the numerical calculations presented in this section, a fraction of ions transferred into the mirror-part is approximately 30%.

When ions suffer from scattering to the mirror-part, ions are not always going through the mirror end. Some of these ions are reflected on the way to the mirror point, if they carry the larger action integral than the critical one for escaping. The criterion for an ion escaping through the mirror point can be given by the inequality:

$$J < \frac{H}{|qB_m|} - \frac{\Omega_m P_\theta}{|qB_m|} \tag{10}$$

for a positive P_θ , where the quantity B_m and Ω_m are the magnetic field and the gyro-frequency of ions, respectively at the mirror point. Example of escaping ions with positive canonical angular momentum P_θ from the magnetic mirror is exhibited in Fig. 7. If an ion has negative canonical angular momentum, on the other hand, the condition for the mirror loss can be represented by:

$$J < \frac{H}{|qB_m|} , \tag{11}$$

that is identical to that for a mirror loss, if one employ Eq. (5) for an off-axis gyrating ion. The boundary of the mirror loss is shown in Fig. 6. The confinement or loss of ions is more complicate due to the electrostatic potential produced by the different behaviors between ions and electrons. We will discuss those problems in the subsequent paper.

We have discussed collisionless stochastic pitch angle scattering of ions only. Since electrons have extremely small mass, their inertia are negligible and the stochastic behavior or the related electron loss can be ignored.

5. Conclusions

Ion motions in the edge region of an FRC have been studied. Numerical calculations showed the following conclusions:

i) The action integral of an ion keeps its value as constant in a regular magnetic field. When the ion passes through the vicinity of an x-point, however, the action integral changes instantaneously. This process can be understood as collisionless stochastic pitch angle scattering.

In the present paper, the process of this pitch angle scattering has been examined. For an ion moving in the cusp-like region, the following results were obtained:

ii) The scattering might be isotropic, since the distribution of the action integral J after the scattering tends to be the one expected analytically.

iii) Correlation coefficients of action integral between before and after the scattering clarified that the branch-transfer from the separatrix-part to the reversal-part or to the mirror-part and their inverse transfer appear to be stochastic.

For an ion moving in the mirror-like region, we have the following results:

iv) As the action integral J increases, then the ion motion tends to be adiabatic.

v) Non-adiabatic ions are observed, if their canonical angular momenta approach to zero. On the other hand, as the absolute value of canonical angular momentum increases, ions move regularly since their guiding center locate far from an x-point.

As a result, one has to take into account the effect of collisionless stochastic pitch angle scattering, that can be appreciable for an ion located near the edge layer of an FRC. A similar phenomena of an electron are safely ignored.

References

(1) H.Momota, Kakuyugo Kenkyu, **61** (1987) 5.

(2) H.Momota and Y.Tomita, Kakuyugo Kenkyu, **67** (1992) 539.

(3) R.E.Siemon, et al., Nucl. Fusion, **9** (1986) 13.

(4) M.Tuszewski, Nucl. Fusion, **28** (1988) 2033.

(5) J.T.Slough, et al., Phys. Rev. Lett., **69** (1992) 2212.

(6) H.Momota, LA-11808-C, Los Alamos National Laboratory, New Mexico, USA (1989) 8.

(7) Y.Tomita, L.Y.Shu, and H.Momota, *Proc. Seventh Int. Conf. on Emerging Nuclear Energy Systems,* Makuhari, Chiba, Japan 20 - 24 September 1993 (1993) p.522.

(8) H.Momota, J. of Japan Institute of Energy, **72** (1993) 91.

(9) H.Momota, et al., Fusion Technol., **21** (1992) 2307 .

(10) H.Momota, et al., *Proc. Seventh Int. Conf. on Emerging Nuclear Energy Systems,* Makuhari, Chiba, Japan 20 - 24 September 1993 (1993) p.16.

(11) M. Y. Hsiao and G. H. Miley, Nucl. Fusion **24**, 1029 (1984).

(12) M. Y. Hsiao and G. H. Miley, Phys. Fluids **28**, 1440 (1985).

(13) M. Y. Hsiao, J. L. Staudenmeier and P. R. Chiang, Phys. Fluids **B 1**, 375 (1989).

(14) J. M. Finn, Plasma Phys **21**, 405 (1979).

(15) M. J. Hill, Philos. Trans. R. Soc., Lond., Ser. A., Pt I, C / XXXV 213 (1894).
(16) R. J. Hastie, G. D. Hobbs and J. B. Taylor, *Proc. 3rd Int. Conf. on Plasma Physics and Controlled Nuclear Fusion Research*, **Vol. 1**, Vienna, 389 (1968)
(17) B. V. Chirikov, Phys. Reports **52**, 263 (1979).

Figure Captions

Fig. 1 Examples of accessible region for 100keV deuteron with relatively small canonical angular momentum P_θ in an FRC. (a) For the positive P_θ, 2.62×10^{-23} [Joule · sec], the particle behavior near the field-null x-point is similar to a magnetic cusp point. Therefore we refer this accessible region as the cusp-like region. (b) For the negative P_θ, -2.62×10^{-21} [Joule · sec], the particle trajectories in this accessible region are off-axis and gyrating which is referred as the mirror-like region.

Fig. 2 An example of time history of the action integral J to particle motion in the cusp-like region of an FRC.

Fig. 3 Correlation diagrams of the action integral between before (J_i) and after (J_f) passing the scattering region in the cusp-like region. These are indicated separately for each transfer,i.e., (a) from separatrix-part to the same one, (b) from separatrix-part to reversal-part, (c) from separatrix-part to mirror-part, (d) from reversal-part to separatrix part, (e) from reversal-part to the same one, and (f) from reversal-part to mirror-part. The correlation coefficients R are also indicated in these diagrams.

Fig. 4 The histograms of the action integral J: (a) after the first scattering and (b) the second scattering in the cusp-like region of an FRC. The solid lines show the distribution scattered isotropically: Eq.(9).

Fig. 5 The ensemble square average $<(\Delta J / J)^2>$ versus action integral J for deuterons in the mirror-like region of an FRC. The total energy and the canonical angular momentum are 100 keV and 2.62×10^{-23} [Joule · sec], respectively.

Fig. 6 Boundary values of the action integral J versus canonical angular momentum P_θ. A particle with larger J than the boundary value plays adiabatic behavior. The boundary of the mirror-loss obtained by Eq.(11) is also indicated by solid line.

Fig. 7 An example of escaping particle from the system. This particle passes through an x-point once again, therefore it is subject to the pitch angle scattering many times. Its action integral satisfies the mirror loss criterion eventually, and then it losses.

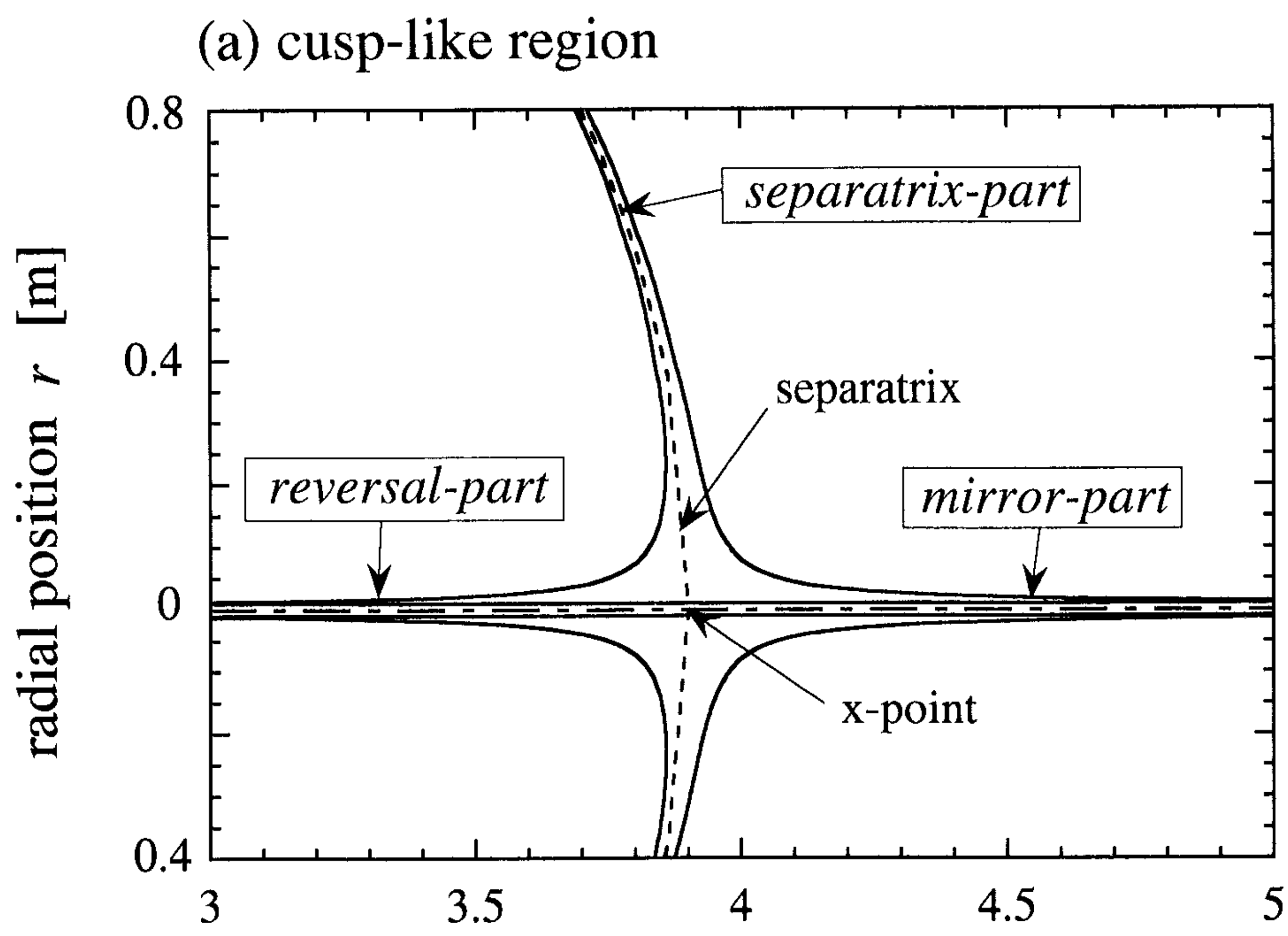
(a) cusp-like region
separatrix-part
separatrix
reversal-part
mirror-part
x-point
0.8
0.4
0
0.4
3
3.5
4
4.5
5
radial position r [m]
axial position z [m]

Fig.1 (a)

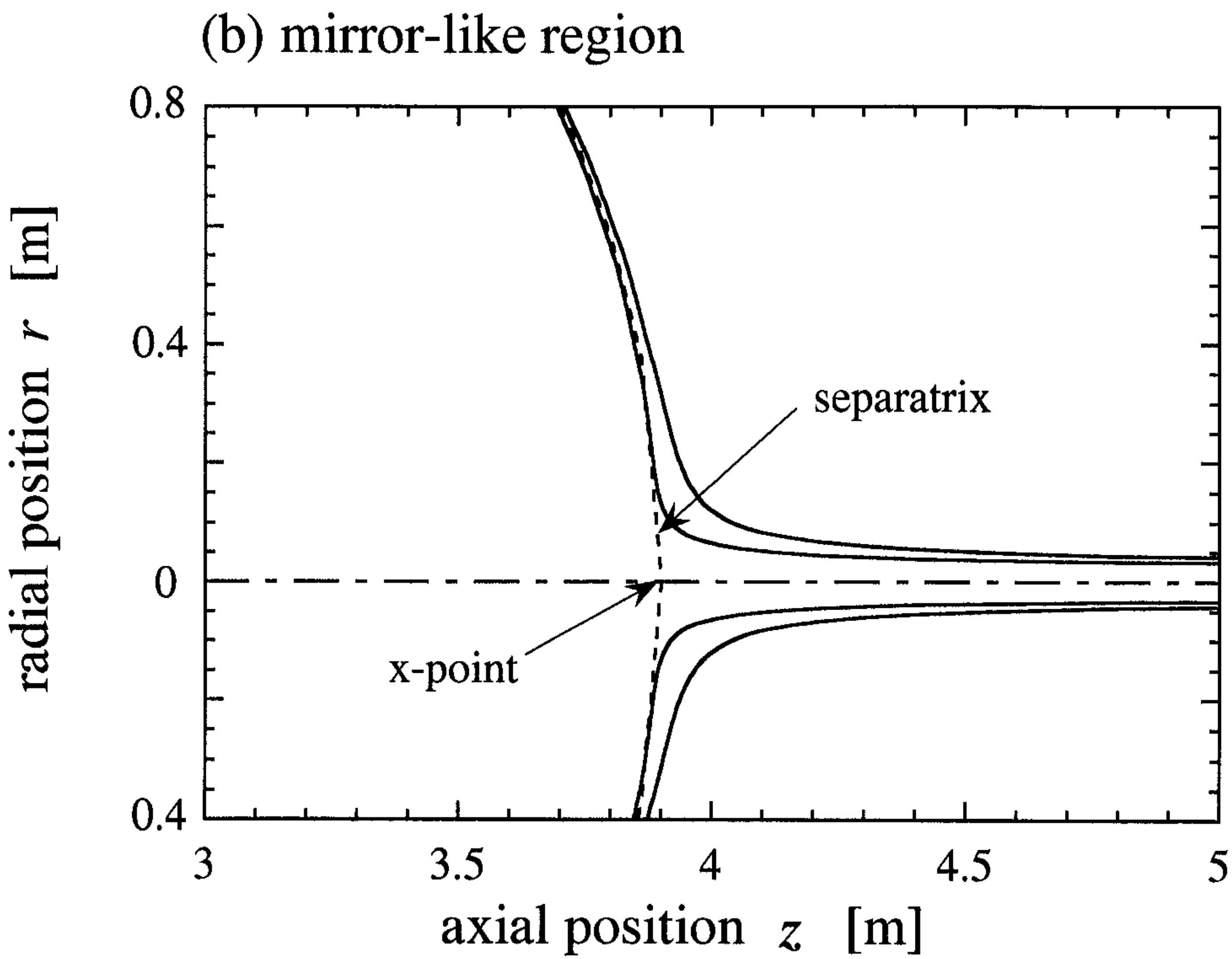
(b) mirror-like region
0.8
0.4
0
0.4
3
3.5
4
4.5
5
separatrix
x-point
radial position r [m]
axial position z [m]

Fig.1 (b)

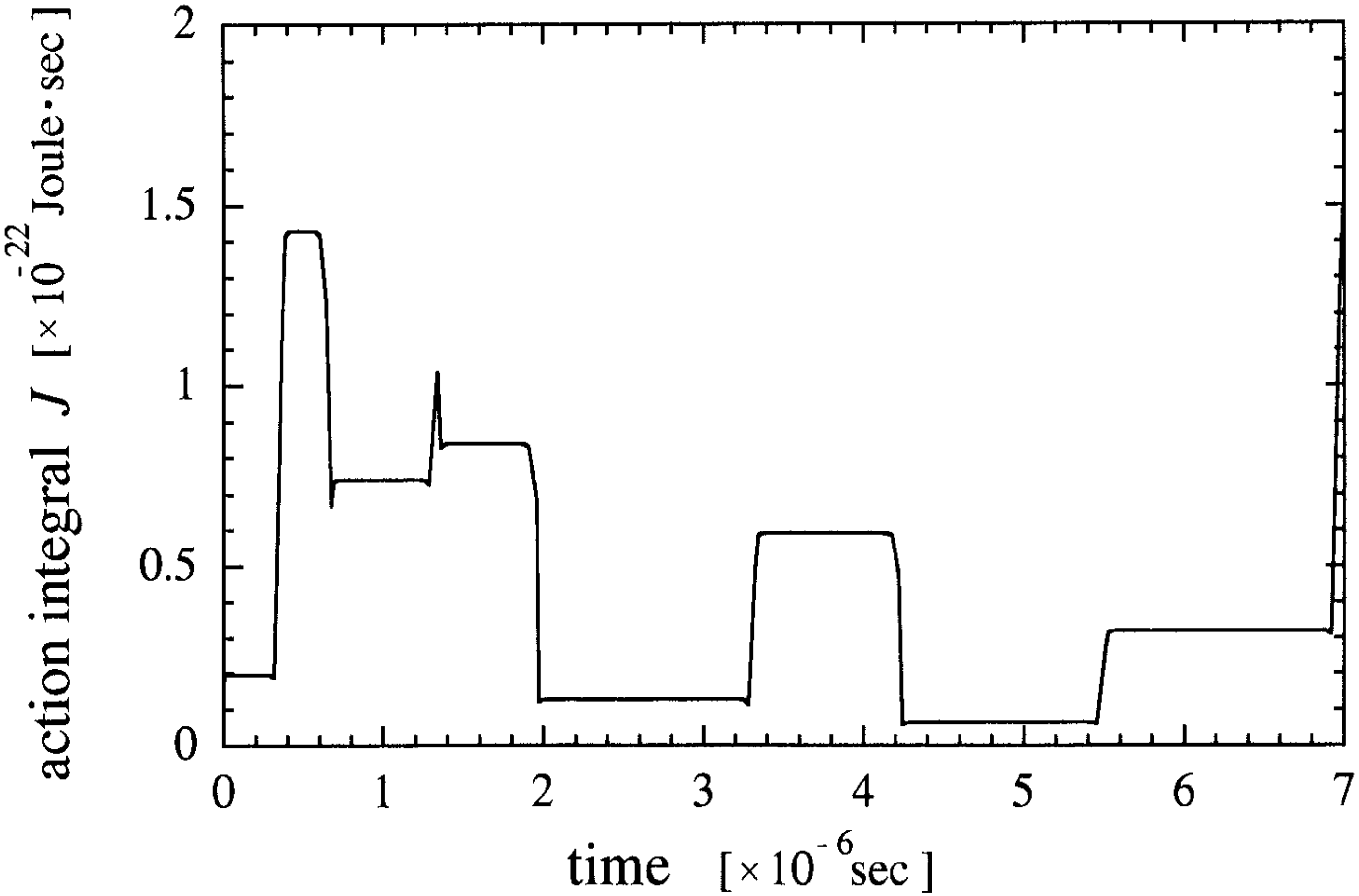
action integral J [×10^-22 Joule·sec]
2
1.5
1
0.5
0
0
1
2
3
4
5
6
7
time [×10^-6 sec]

Fig.2

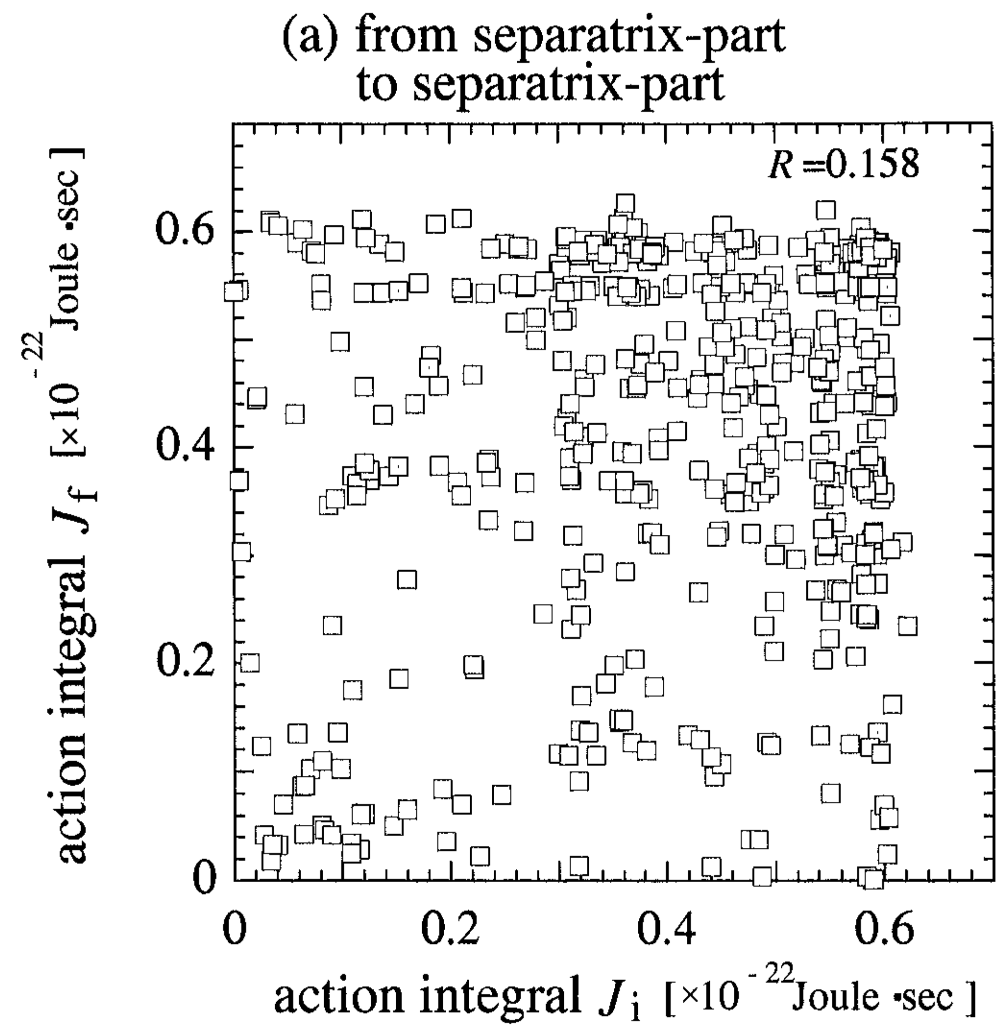
(a) from separatrix-part
to separatrix-part
R =0.158
0.6
0.4
0.2
0
0
0.2
0.4
0.6
action integral J_f [×10^-22 Joule •sec]
action integral J_i [×10^-22 Joule •sec]

Fig.3 (a)

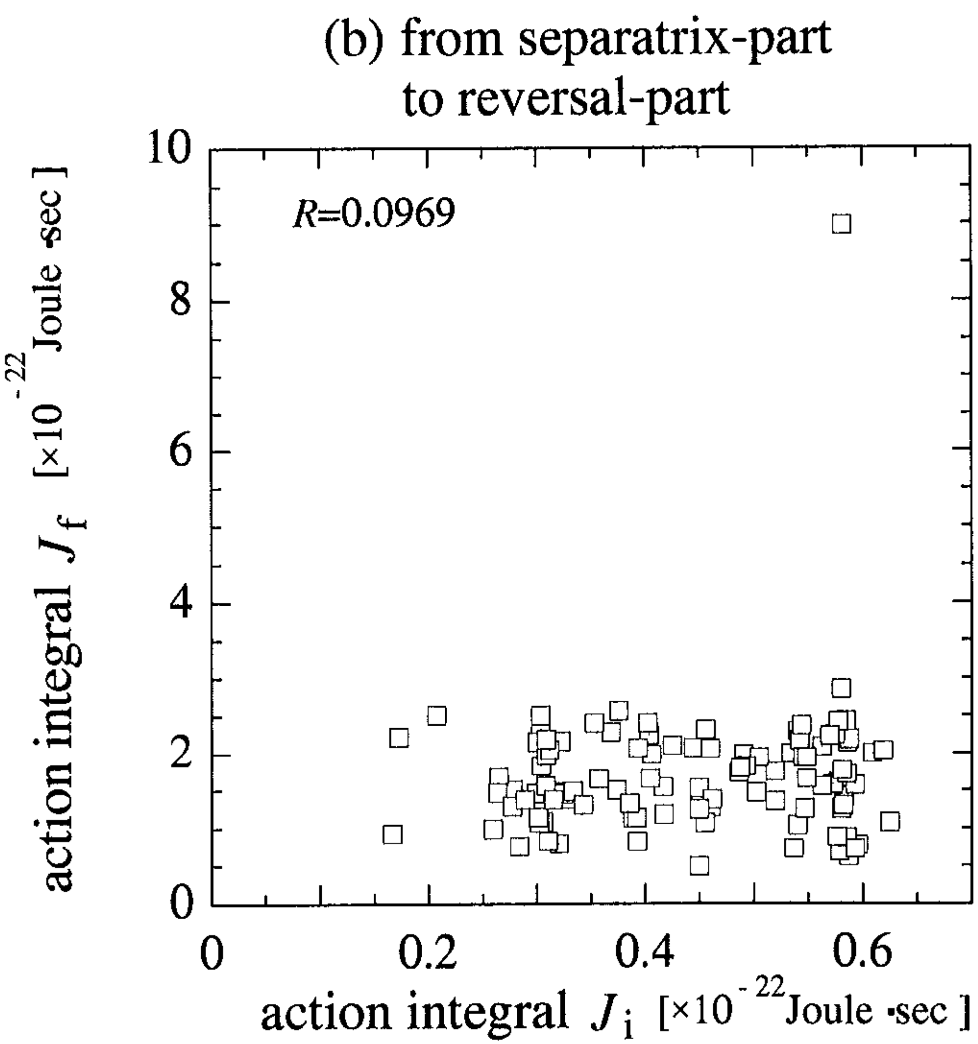
(b) from separatrix-part
to reversal-part
R=0.0969
10
8
6
4
2
0
0
0.2
0.4
0.6
action integral J_f [×10^{-22}Joule ·sec]
action integral J_i [×10^{-22}Joule ·sec]

Fig.3 (b)

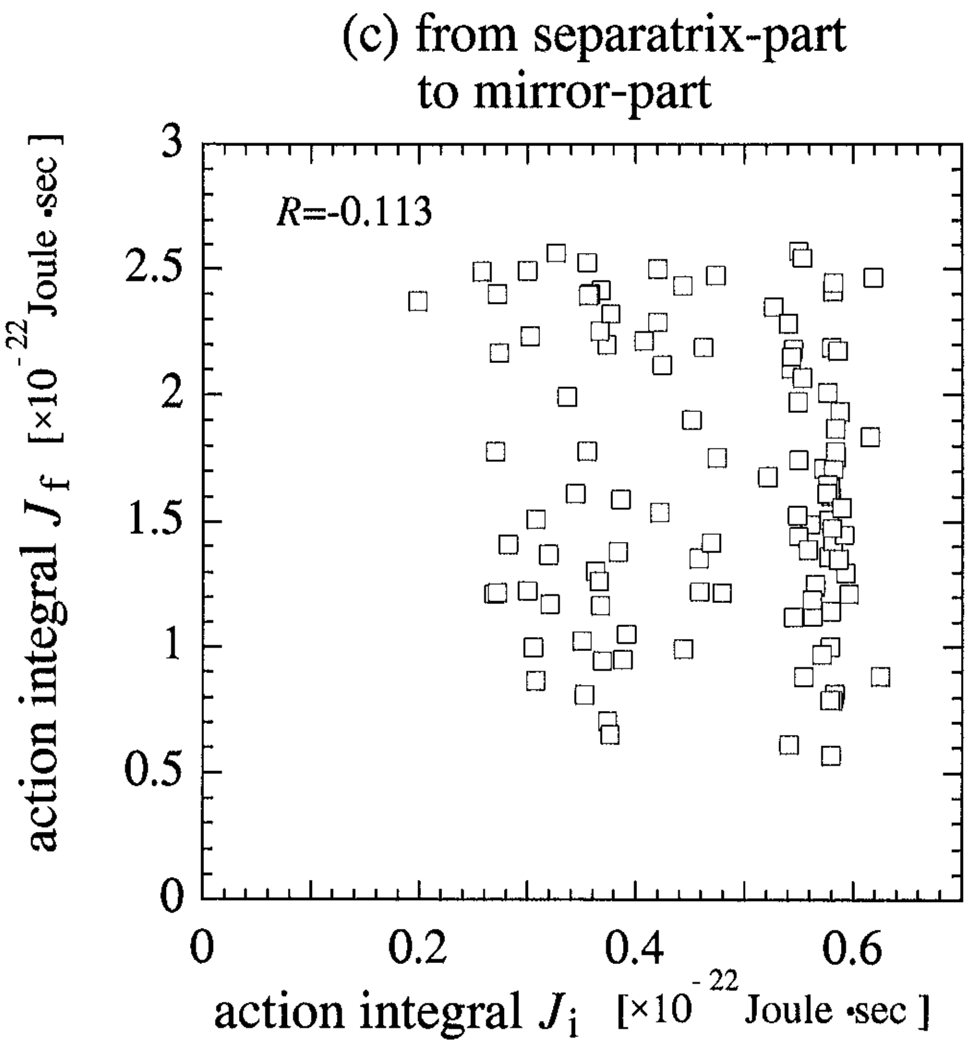
(c) from separatrix-part
to mirror-part
R=-0.113
action integral J_f [×10^-22 Joule ·sec]
action integral J_i [×10^-22 Joule ·sec]
3
2.5
2
1.5
1
0.5
0
0.2
0.4
0.6

Fig.3 (c)

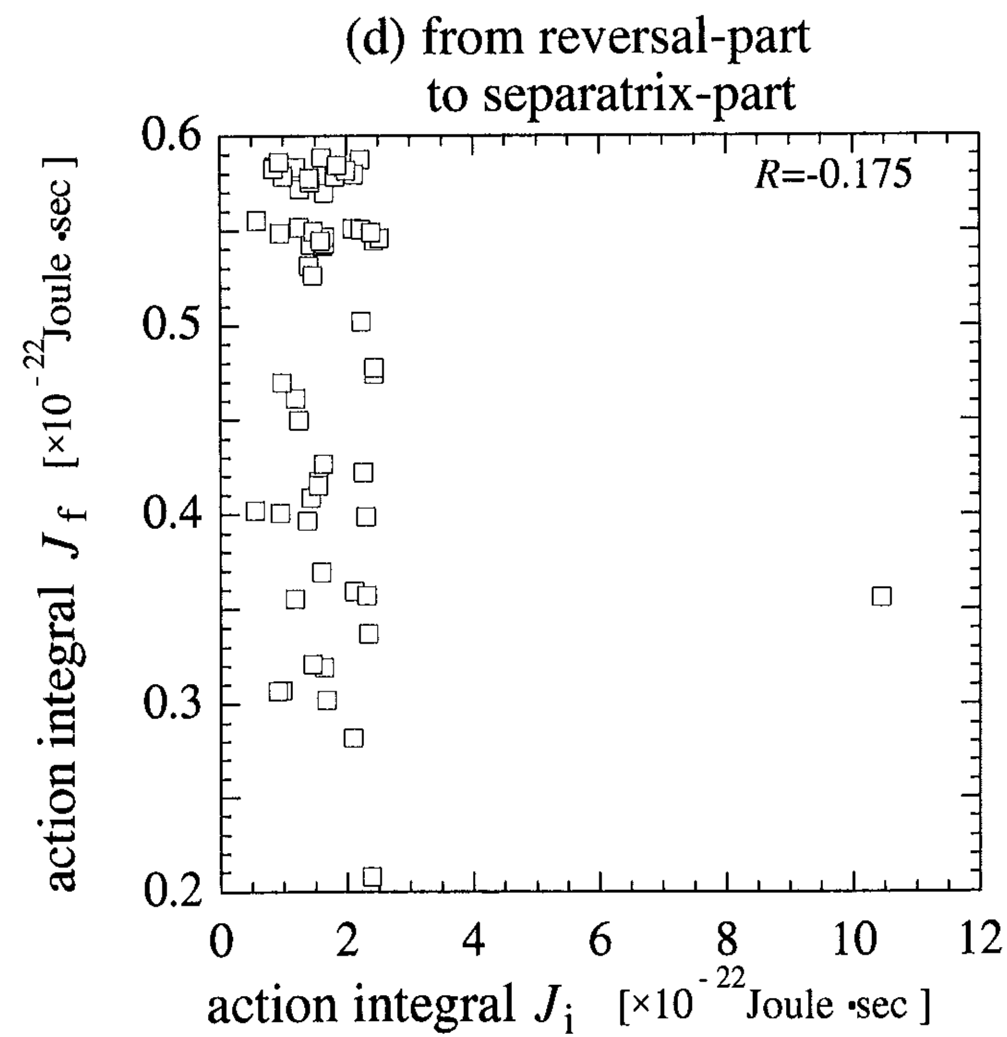
(d) from reversal-part
to separatrix-part
R=-0.175
0.6
0.5
0.4
0.3
0.2
0
2
4
6
8
10
12
action integral J f [×10 - 22 Joule •sec]
action integral J i [×10 - 22 Joule •sec]

Fig.3 (d)

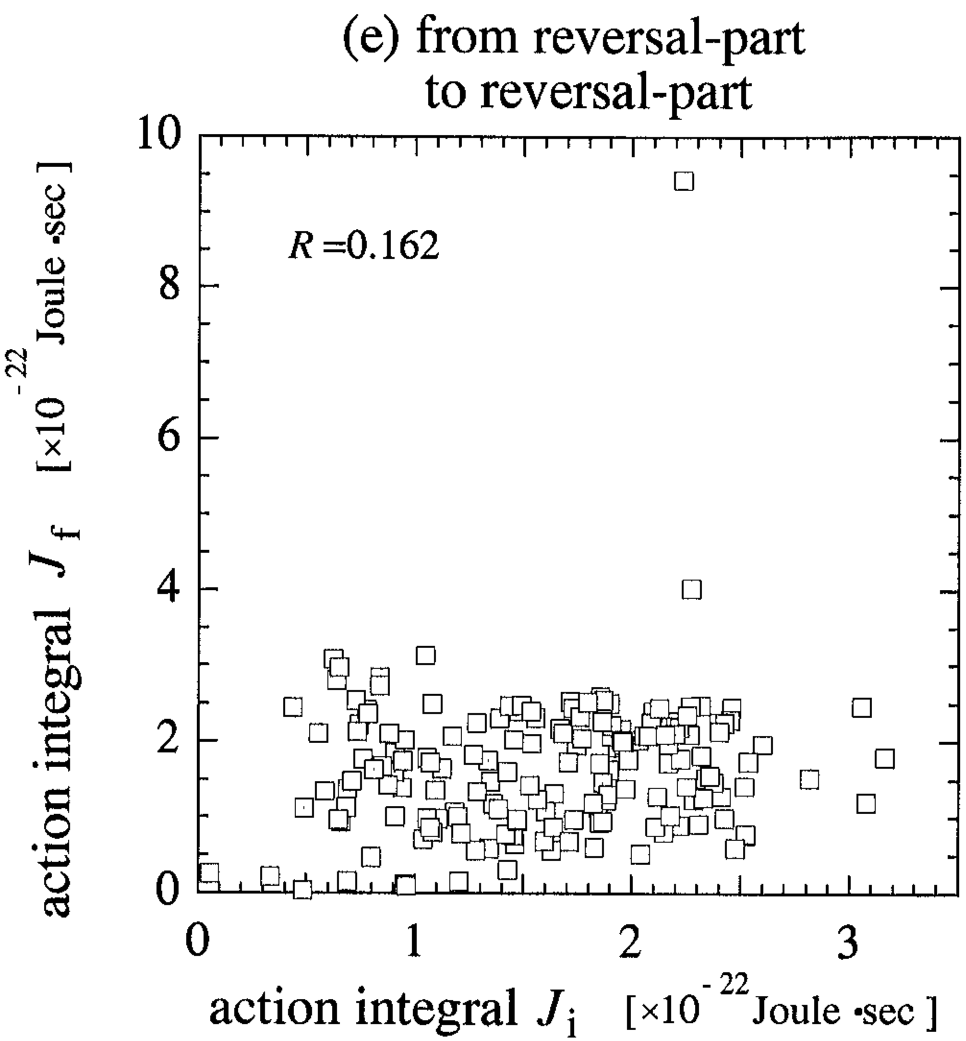
(e) from reversal-part
to reversal-part
R =0.162
action integral J_f [×10^-22 Joule ·sec]
action integral J_i [×10^-22 Joule ·sec]
0
2
4
6
8
10
0
1
2
3

Fig.3 (e)

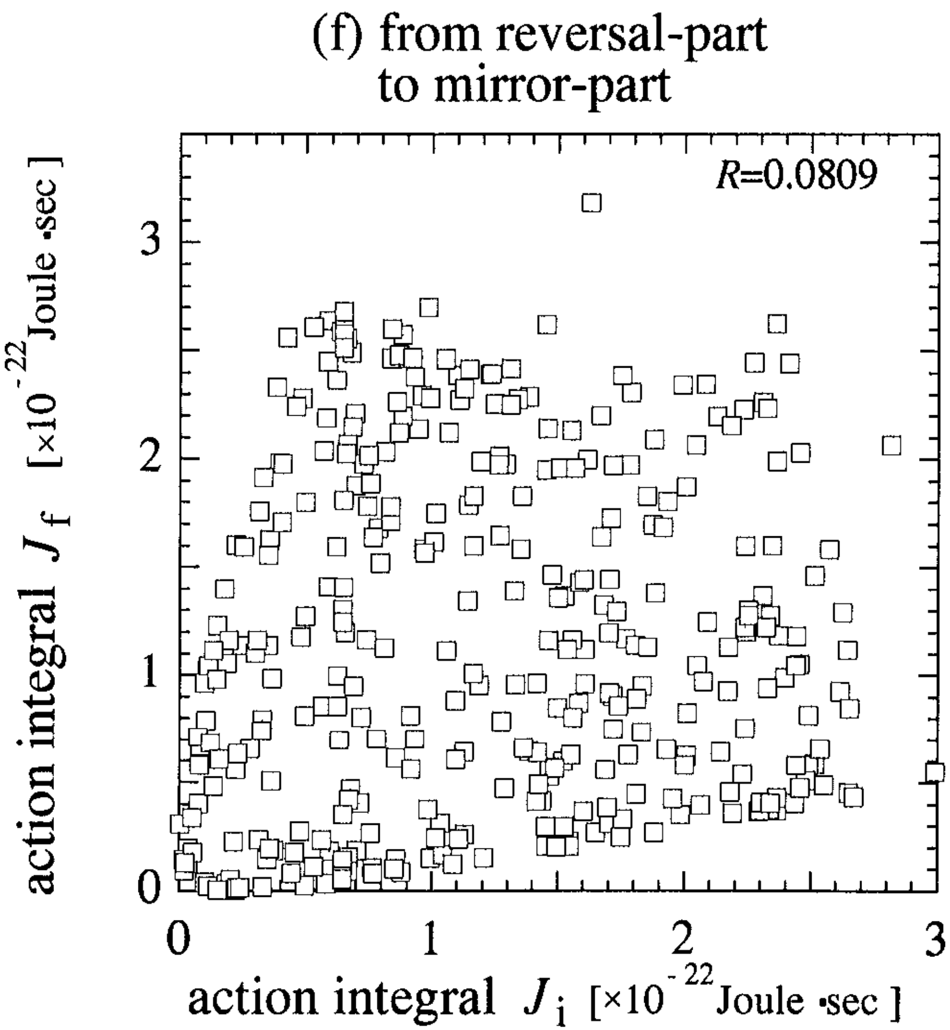
(f) from reversal-part
to mirror-part
R=0.0809
action integral J f [×10^-22 Joule ·sec]
action integral J i [×10^-22 Joule ·sec]
0
1
2
3
0
1
2
3

Fig.3 (f)

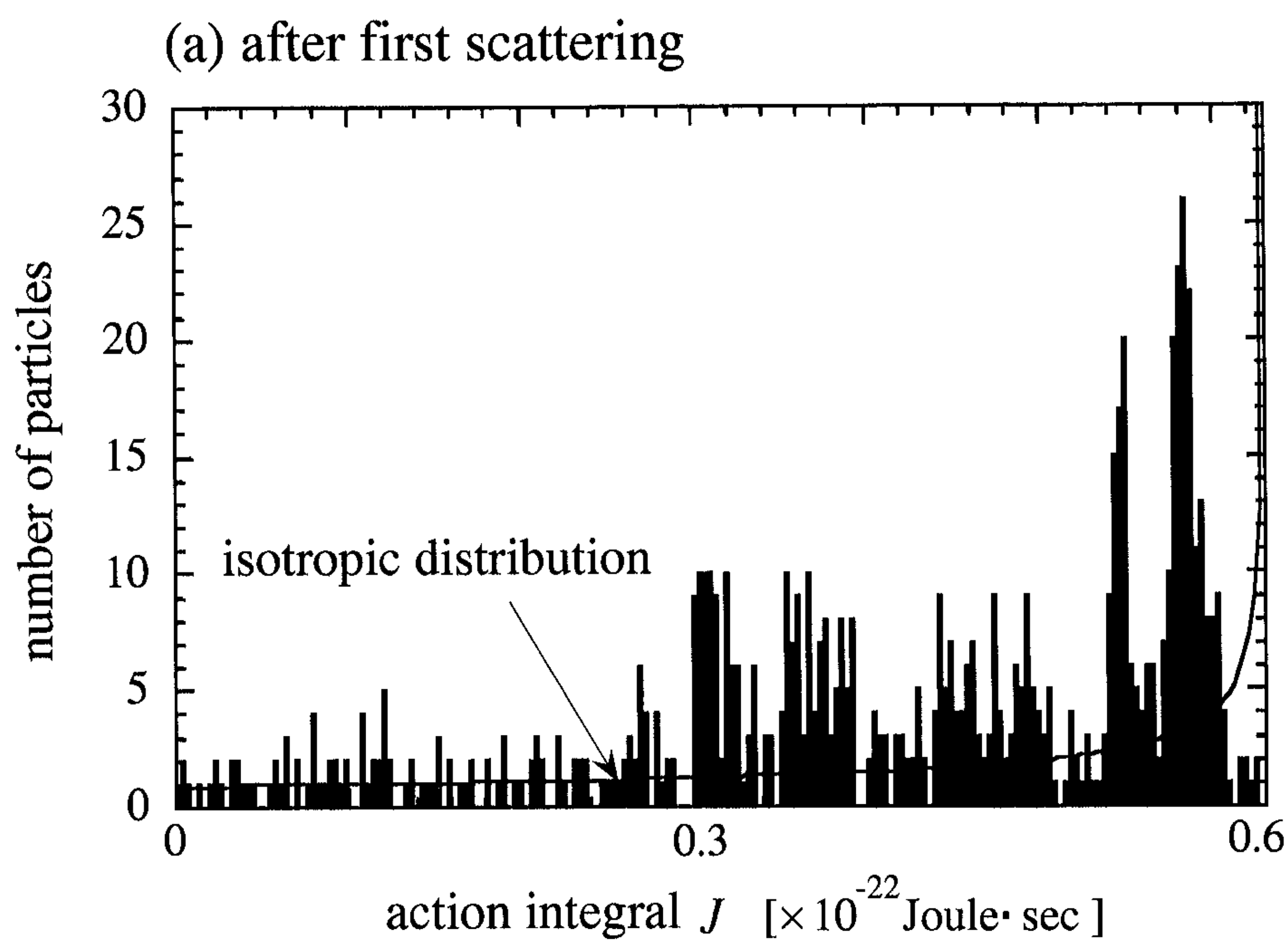
(a) after first scattering
30
25
20
15
10
5
0
number of particles
isotropic distribution
0
0.3
0.6
action integral J [×10^-22 Joule· sec]

Fig.4 (a)

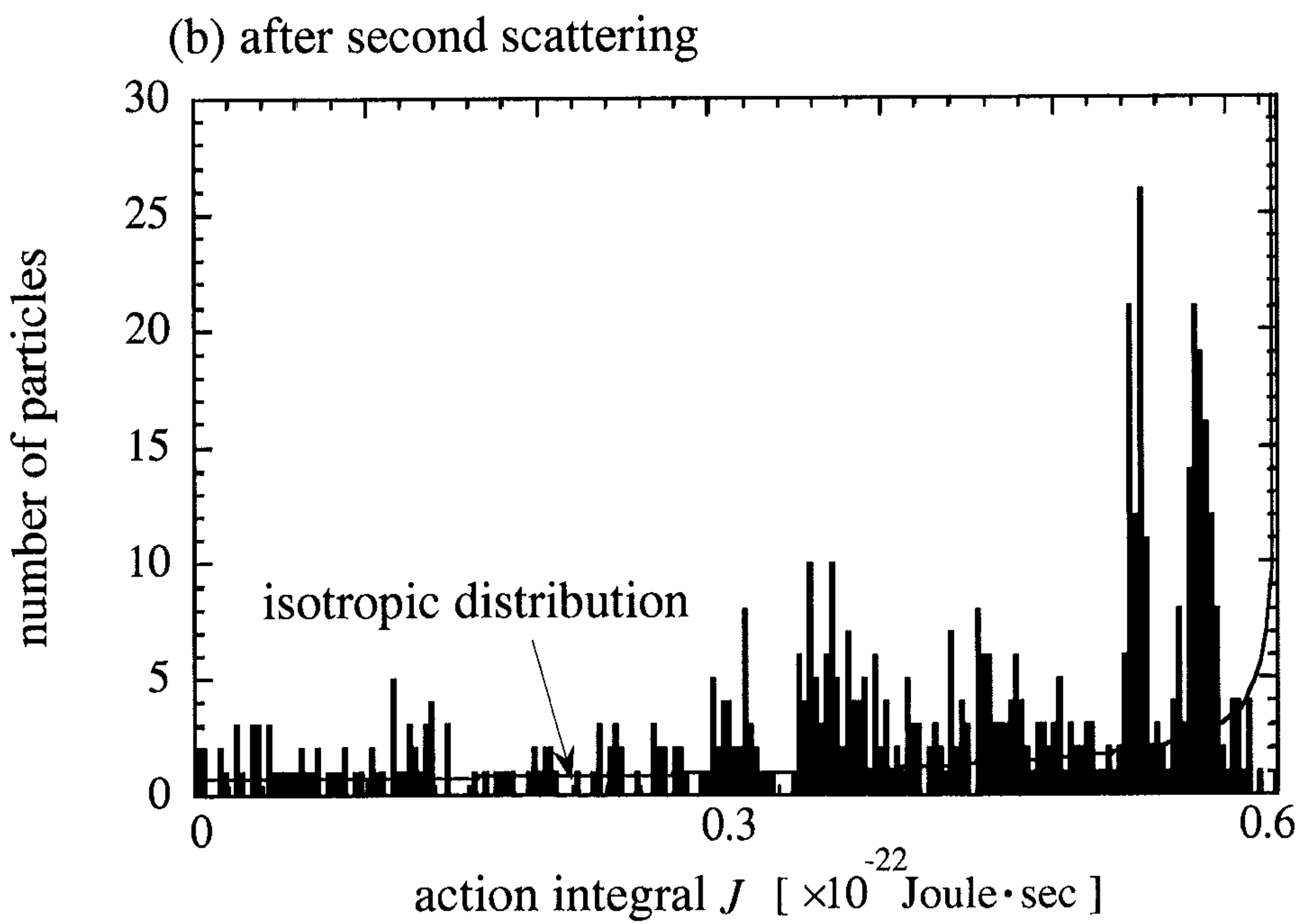

(b) after second scattering
30
25
20
15
10
5
0
number of particles
isotropic distribution
0
0.3
0.6
action integral J [×10^-22 Joule・sec]

Fig.4 (b)

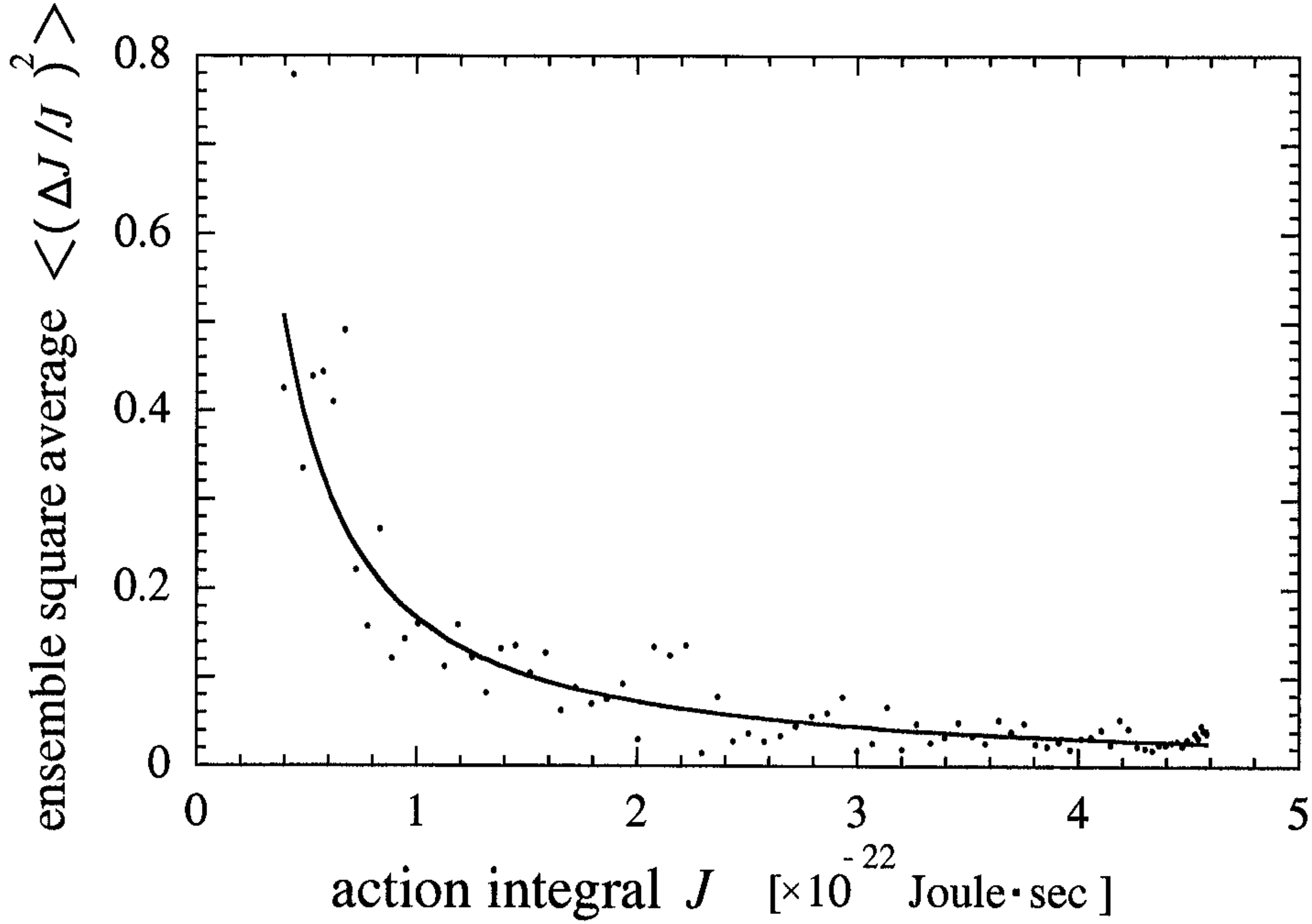
ensemble square average <(ΔJ /J)²>
0.8
0.6
0.4
0.2
0
0
1
2
3
4
5
action integral J [×10⁻²² Joule·sec]

Fig.5

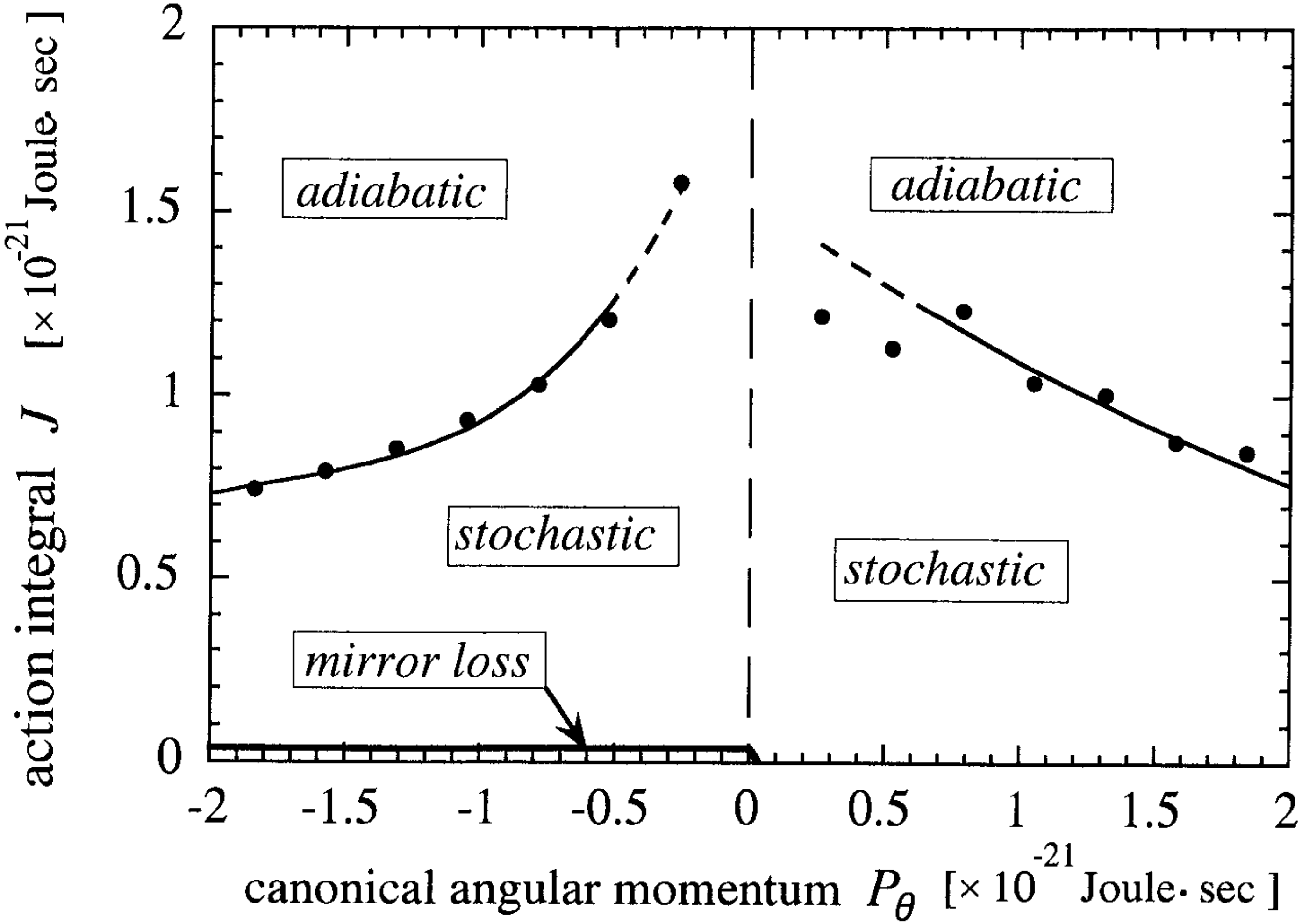
adiabatic
adiabatic
stochastic
stochastic
mirror loss
action integral J [× 10^-21 Joule· sec]
canonical angular momentum P_θ [× 10^-21 Joule· sec]
2
1.5
1
0.5
0
-2
-1.5
-1
-0.5
0
0.5
1
1.5
2

Fig.6

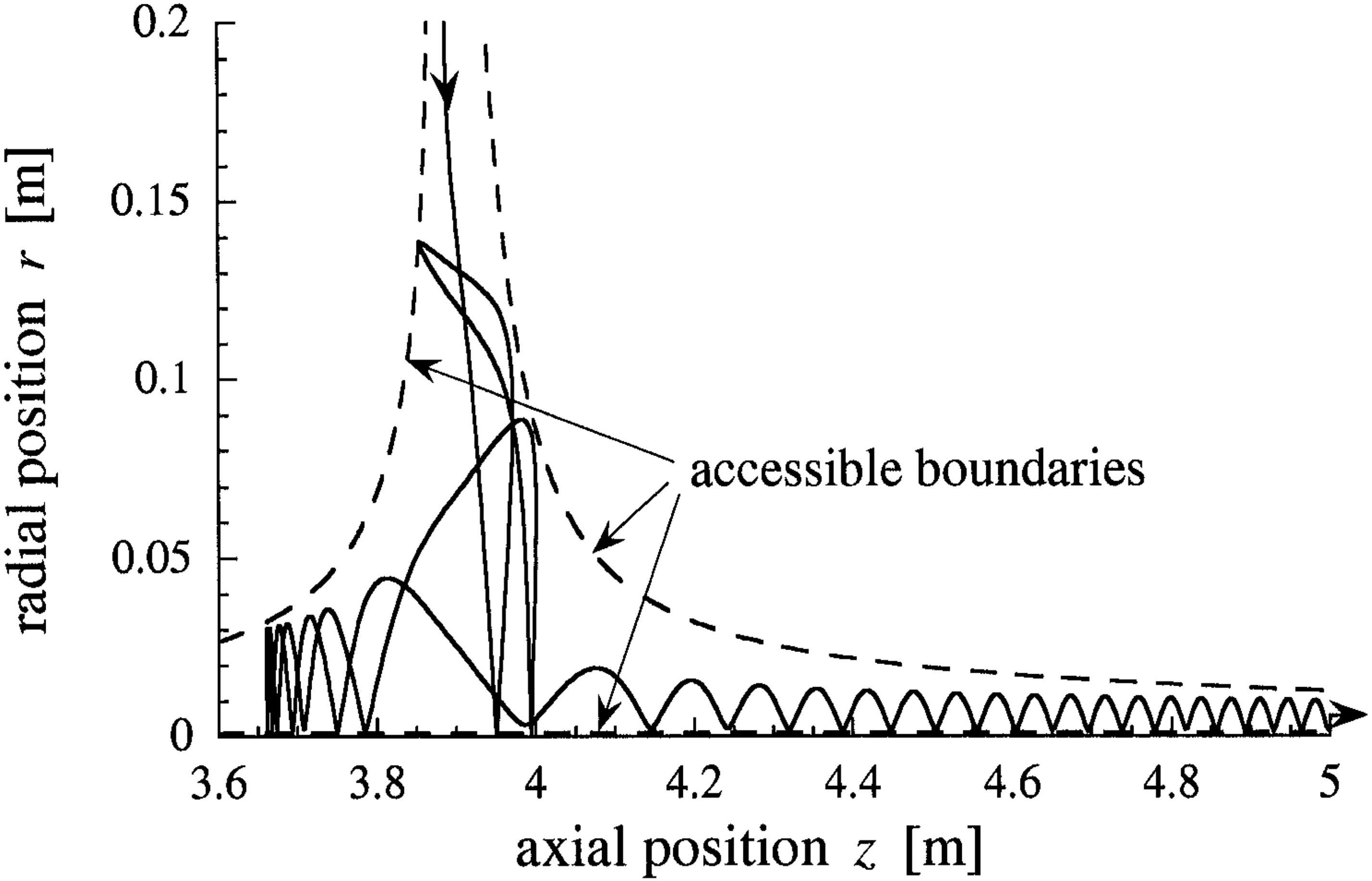
0.2
0.15
0.1
0.05
0
radial position r [m]
accessible boundaries
3.6
3.8
4
4.2
4.4
4.6
4.8
5
axial position z [m]

Fig.7

Recent Issues of NIFS Series

NIFS-451 J. Li, X. Gong, L. Luo, F.X. Yin, N. Noda, B. Wan, W. Xu, X. Gao, F. Yin, J.G. Jiang, Z. Wu., J.Y. Zhao, M. Wu, S. Liu and Y. Han,
Effects of High Z Probe on Plasma Behavior in HT-6M Tokamak; Sep. 1996

NIFS-452 N. Nakajima, K. Ichiguchi, M. Okamoto and R.L. Dewar,
Ballooning Modes in Heliotrons/Torsatrons; Sep. 1996 (IAEA-CN-64/D3-6)

NIFS-453 A. Iiyoshi,
Overview of Helical Systems; Sep. 1996 (IAEA-CN-64/O1-7)

NIFS-454 S. Saito, Y. Nomura, K. Hirose and Y.H. Ichikawa,
Separatrix Reconnection and Periodic Orbit Annihilation in the Harper Map; Oct. 1996

NIFS-455 K. Ichiguchi, N. Nakajima and M. Okamoto,
Topics on MHD Equilibrium and Stability in Heliotron / Torsatron; Oct. 1996

NIFS-456 G. Kawahara, S. Kida, M. Tanaka and S. Yanase,
Wrap, Tilt and Stretch of Vorticity Lines around a Strong Straight Vortex Tube in a Simple Shear Flow; Oct. 1996

NIFS-457 K. Itoh, S.- I. Itoh, A. Fukuyama and M. Yagi,
Turbulent Transport and Structural Transition in Confined Plasmas; Oct. 1996

NIFS-458 A. Kageyama and T. Sato,
Generation Mechanism of a Dipole Field by a Magnetohydrodynamic Dynamo; Oct. 1996

NIFS-459 K. Araki, J. Mizushima and S. Yanase,
The Non-axisymmetric Instability of the Wide-Gap Spherical Couette Flow; Oct. 1996

NIFS-460 Y. Hamada, A. Fujisawa, H. Iguchi, A. Nishizawa and Y. Kawasumi,
A Tandem Parallel Plate Analyzer; Nov. 1996

NIFS-461 Y. Hamada, A. Nishizawa, Y. Kawasumi, A. Fujisawa, K. Narihara, K. Ida, A. Ejiri, S. Ohdachi, K. Kawahata, K. Toi, K. Sato, T. Seki, H. Iguchi, K. Adachi, S. Hidekuma, S.Hirokura, K. Iwasaki, T. Ido, M. Kojima, J. Koong, R. Kumazawa, H. Kuramoto, T. Minami, I. Nomura, H. Sakakita, M. Sasao, K.N. Sato, T. Tsuzuki, J. Xu, I. Yamada and T. Watari,
Density Fluctuation in JIPP T-IIU Tokamak Plasmas Measured by a Heavy Ion Beam Probe; Nov. 1996

NIFS-462 N. Katsuragawa, H. Hojo and A. Mase,
Simulation Study on Cross Polarization Scattering of Ultrashort-Pulse

Electromagnetic Waves; Nov. 1996

NIFS-463 V. Voitsenya, V. Konovalov, O. Motojima, K. Narihara, M. Becker and B. Schunke, *Evaluations of Different Metals for Manufacturing Mirrors of Thomson Scattering System for the LHD Divertor Plasma*; Nov. 1996

NIFS-464 M. Pereyaslavets, M. Sato, T. Shimozuma, Y. Takita, H. Idei, S. Kubo, K. Ohkubo and K. Hayashi, *Development and Simulation of RF Components for High Power Millimeter Wave Gyrotrons*; Nov. 1996

NIFS-465 V.S. Voitsenya, S. Masuzaki, O. Motojima, N. Noda and N. Ohyabu, *On the Use of CX Atom Analyzer for Study Characteristics of Ion Component in a LHD Divertor Plasma*; Dec. 1996

NIFS-466 H. Miura and S. Kida, *Identification of Tubular Vortices in Complex Flows*; Dec. 1996

NIFS-467 Y. Takeiri, Y. Oka, M. Osakabe, K. Tsumori, O. Kaneko, T. Takanashi, E. Asano, T. Kawamoto, R. Akiyama and T. Kuroda, *Suppression of Accelerated Electrons in a High-current Large Negative Ion Source*; Dec. 1996

NIFS-468 A. Sagara, Y. Hasegawa, K. Tsuzuki, N. Inoue, H. Suzuki, T. Morisaki, N. Noda, O. Motojima, S. Okamura, K. Matsuoka, R. Akiyama, K. Ida, H. Idei, K. Iwasaki, S. Kubo, T. Minami, S. Morita, K. Narihara, T. Ozaki, K. Sato, C. Takahashi, K. Tanaka, K. Toi and I. Yamada, *Real Time Boronization Experiments in CHS and Scaling for LHD*; Dec. 1996

NIFS-469 V.L. Vdovin, T.Watari and A. Fukuyama, *3D Maxwell-Vlasov Boundary Value Problem Solution in Stellarator Geometry in Ion Cyclotron Frequency Range (final report)*; Dec. 1996

NIFS-470 N. Nakajima, M. Yokoyama, M. Okamoto and J. Nührenberg, *Optimization of M=2 Stellarator*; Dec. 1996

NIFS-471 A. Fujisawa, H. Iguchi, S. Lee and Y. Hamada, *Effects of Horizontal Injection Angle Displacements on Energy Measurements with Parallel Plate Energy Analyzer*; Dec. 1996

NIFS-472 R. Kanno, N. Nakajima, H. Sugama, M. Okamoto and Y. Ogawa, *Effects of Finite-β and Radial Electric Fields on Neoclassical Transport in the Large Helical Device;* Jan. 1997

NIFS-473 S. Murakami, N. Nakajima, U. Gasparino and M. Okamoto, *Simulation Study of Radial Electric Field in CHS and LHD*; Jan. 1997

NIFS-474 K. Ohkubo, S. Kubo, H. Idei, M. Sato, T. Shimozuma and Y. Takita, *Coupling of Tilting Gaussian Beam with Hybrid Mode in the Corrugated*

Waveguide; Jan. 1997

NIFS-475 A. Fujisawa, H. Iguchi, S. Lee and Y. Hamada,
Consideration of Fluctuation in Secondary Beam Intensity of Heavy Ion Beam Prove Measurements; Jan. 1997

NIFS-476 Y. Takeiri, M. Osakabe, Y. Oka, K. Tsumori, O. Kaneko, T. Takanashi, E. Asano, T. Kawamoto, R. Akiyama and T. Kuroda,
Long-pulse Operation of a Cesium-Seeded High-Current Large Negative Ion Source; Jan. 1997

NIFS-477 H. Kuramoto, K. Toi, N. Haraki, K. Sato, J. Xu, A. Ejiri, K. Narihara, T. Seki, S. Ohdachi, K. Adati, R. Akiyama, Y. Hamada, S. Hirokura, K. Kawahata and M. Kojima,
Study of Toroidal Current Penetration during Current Ramp in JIPP T-IIU with Fast Response Zeeman Polarimeter; Jan., 1997

NIFS-478 H. Sugama and W. Horton,
Neoclassical Electron and Ion Transport in Toroidally Rotating Plasmas; Jan. 1997

NIFS-479 V.L. Vdovin and I.V. Kamenskij,
3D Electromagnetic Theory of ICRF Multi Port Multi Loop Antenna; Jan. 1997

NIFS-480 W.X. Wang, M. Okamoto, N. Nakajima, S Murakami and N. Ohyabu,
Cooling Effect of Secondary Electrons in the High Temperature Divertor Operation; Feb. 1997

NIFS-481 K. Itoh, S.-I. Itoh, H. Soltwisch and H.R. Koslowski,
Generation of Toroidal Current Sheet at Sawtooth Crash; Feb. 1997

NIFS-482 K. Ichiguchi,
Collisionality Dependence of Mercier Stability in LHD Equilibria with Bootstrap Currents; Feb. 1997

NIFS-483 S. Fujiwara and T. Sato,
Molecular Dynamics Simulations of Structural Formation of a Single Polymer Chain: Bond-orientational Order and Conformational Defects; Feb. 1997

NIFS-484 T. Ohkawa,
Reduction of Turbulence by Sheared Toroidal Flow on a Flux Surface; Feb. 1997

NIFS-485 K. Narihara, K. Toi, Y. Hamada, K. Yamauchi, K. Adachi, I. Yamada, K. N. Sato, K. Kawahata, A. Nishizawa, S. Ohdachi, K. Sato, T. Seki, T. Watari, J. Xu, A. Ejiri, S. Hirokura, K. Ida, Y. Kawasumi, M. Kojima, H. Sakakita, T. Ido, K. Kitachi, J. Koog and H. Kuramoto,
Observation of Dusts by Laser Scattering Method in theJIPPT-IIU Tokamak Mar. 1997

NIFS-486 S. Bazdenkov, T. Sato and The Complexity Simulation Group,
Topological Transformations in Isolated Straight Magnetic Flux Tube; Mar. 1997

NIFS-487 M. Okamoto,
Configuration Studies of LHD Plasmas; Mar. 1997

NIFS-488 A. Fujisawa, H. Iguchi, H. Sanuki, K. Itoh, S. Lee, Y. Hamada, S. Kubo, H. Idei, R. Akiyama, K. Tanaka, T. Minami, K. Ida, S. Nishimura, S. Morita, M. Kojima, S. Hidekuma, S.-I. Itoh, C. Takahashi, N. Inoue, H. Suzuki, S. Okamura and K. Matsuoka,
Dynamic Behavior of Potential in the Plasma Core of the CHS Heliotron/Torsatron; Apr. 1997

NIFS-489 T. Ohkawa,
Pfirsch - Schlüter Diffusion with Anisotropic and Nonuniform Superthermal Ion Pressure; Apr. 1997

NIFS-490 S. Ishiguro and The Complexity Simulation Group,
Formation of Wave-front Pattern Accompanied by Current-driven Electrostatic Ion-cyclotron Instabilities; Apr. 1997

NIFS-491 A. Ejiri, K. Shinohara and K. Kawahata,
An Algorithm to Remove Fringe Jumps and its Application to Microwave Reflectometry; Apr. 1997

NIFS-492 K. Ichiguchi, N. Nakajima, M. Okamoto,
Bootstrap Current in the Large Helical Device with Unbalanced Helical Coil Currents; Apr. 1997

NIFS-493 S. Ishiguro, T. Sato, H. Takamaru and The Complexity Simulation Group,
V-shaped dc Potential Structure Caused by Current-driven Electrostatic Ion-cyclotron Instability; May 1997

NIFS-494 K. Nishimura, R. Horiuchi, T. Sato,
Tilt Stabilization by Energetic Ions Crossing Magnetic Separatrix in Field-Reversed Configuration; June 1997

NIFS-495 T. -H. Watanabe and T. Sato,
Magnetohydrodynamic Approach to the Feedback Instability; July 1997

NIFS-496 K. Itoh, T. Ohkawa, S. -I. Itoh, M. Yagi and A. Fukuyama
Suppression of Plasma Turbulence by Asymmetric Superthermal Ions; July 1997

NIFS-497 T. Takahashi, Y. Tomita, H. Momota and Nikita V. Shabrov,
Collisionless Pitch Angle Scattering of Plasma Ions at the Edge Region of an FRC; July 1997